LAMONT-DOHERTY GEOLOGICAL OBSERVATORY
of Columbia University
Palisades, New York, 10964

*

LUNAR HEAT FLOW EXPERIMENT

*

LONG TERM TEMPERATURE OBSERVATIONS
ON THE LUNAR SURFACE AT APOLLO SITES 15 AND 17

by

Kenneth Peters
Marcus G. Langseth, Principal Investigator

October 1975

*

LAMONT-DOHERTY GEOLOGICAL OBSERVATORY
of Columbia University
Palisades, New York, 10964

*

Technical Report No. 3-CU-3-75
National Aeronautics and Space Administration
Contract NAS 9-6037

LUNAR HEAT FLOW EXPERIMENT

*

LONG TERM TEMPERATURE OBSERVATIONS
ON THE LUNAR SURFACE AT APOLLO SITES 15 AND 17

by

Kenneth Peters
Marcus G. Langseth, Principal Investigator

October 1975

*

TABLE OF CONTENTS

TABLE

ILLUSTRATIONS

APPENDIX

*

Abstract

Several investigators of the Apollo lunar experiments have observed gradual increases in the mean temperatures recorded by various surface thermometers. Similar effects have been noticed in the temperatures of the thermometers of the Apollo 15 and 17 Heat Flow Experiments. This report discusses an analysis of the long term temperature histories of the heat flow experiment thermometers. These data show that no change in mean surface temperature at the Apollo 15 and 17 sites has occurred, and suggest that the slow increase in "mean" temperatures of thermometers in the electronics housing are due to changes in radiative properties of the housing's surfaces.

Introduction

Accurate sets of thermometers were placed on the moon as part of the Lunar Heat Flow Experiments. One experiment was installed at the Apollo 15 site at Rima Hadley, in July 1971, and one at the Apollo 17 site in Taurus Littrow, in December 1972. All of these thermometers have been returning data to earth since they were installed on the moon, and provide us with records of temperature variation over a 3.5 and a 2 year period. Some of the Heat Flow Experiment thermometers are above the lunar surface and assume temperatures that satisfy a heat balance between impinging thermal radiation from the sun and the lunar surface, and that lost by radiation to space. These thermometers experience very large variations in temperature throughout a lunation and during eclipses (References 1 and 2). The amplitudes of these monthly variations show a strong annual modulation and additional weaker modulations over much longer times. In this report we describe long term variations that have been observed and compare them with the variations expected.

One of the Heat Flow Experiments' sensors is inside the electronics box housing. The temperatures of this sensor show an annual variation and a slow increase in mean temperature with time.

Measurements:

Thermometers used for the lunar heat flow measurements are contained in slender probes placed in predrilled holes in the lunar soil and in the cables connecting the probes to the electronics unit. Each probe contains eight platinum resistance thermometers. There are four thermocouple junctions in each cable, which are located at distances of approximately 0, 0.65, 1.15 and 1.65 m from the topmost platinum thermometer in the probe, see Figure 1. The electronics are contained in a thermally controlled housing. Another platinum resistance thermometer, the reference thermometer, is attached to the radiator plate of this housing. The reference junctions of all of the thermocouples are thermally connected to the reference thermometer. Thermocouple no. 1 is inside the topmost platinum resistance thermometer in the probe; thus, this platinum thermometer provides a second reference. Table 1 (from Reference 3) shows the absolute accuracy and range of these thermometers.

Figure 2 shows the emplacement of the probes at the Apollo 15 and Apollo 17 sites. At Apollo 15 the holes could be drilled to only half the intended depth and, consequently, many of the thermocouples in the cable were left exposed above the surface. At probe 1 thermocouple no. 4 is inside the portion of the borestem above the surface. At Apollo 17 the holes were drilled to the desired depth and only thermocouple no. 2 is exposed above the surface.

In normal operation, the temperatures of the heat flow experiment thermometers are transmitted to earth every 7.25 minutes. Typical thermocouple temperature variations during a lunation cycle are shown in the inset in Figure 3. For each sensor two temperatures are selected from a lunation cycle and used to examine the long term variations:

1) The maximum temperature near lunar noon, and

2) the temperature at a prescribed time after lunar sunset which we call the "presunrise temperature".

The prescribed times used are 14 days for Apollo 17 and 15 days for Apollo 15, which are just before lunar sunrise and, consequently, these temperatures are near the minimum values for each lunation.

Results of Thermocouple Measurements Above the Lunar Surface

Temperature variations for three typical thermocouples are shown in Figure 3. Daytime maxima for these thermocouples show the dominating character of the annual component of the insolation. The modulating envelopes of the annual variations are, in general, different for each thermocouple, and depend on the orientation of the cable that surrounds the thermocouple. The effect of cable orientation can be seen

in the temperature variations during a lunation (see Figure 3, inset).
The individual thermocouples reach their maximum temperatures at
different times in the lunation. The cable element around thermocouple
no. 2, at A-17, is oriented nearly north-south and has a nearly symmetric
curve relative to lunar noon. Thermocouple no. 4 at A-15 is in the bore-
stem projecting above the surface. The borestem tilts slightly toward the
east. This orientation results in a relatively flat curve that peaks early
in the afternoon. The fact that the temperatures of thermocouple no. 2,
at A-15, peak in the afternoon and are substantially colder than the other
thermometers in the lunar morning indicates that the cable axis orien-
tation at this junction is roughly northwest-southeast and is elevated to the
southeast.

Presunrise temperatures of all thermocouples are much more
constant with time although there is a small annual variation of about half
a degree peak to peak. Mean presunrise temperatures show no detectable
drift, except for an abrupt increase in Apollo 15 temperatures between
lunation 18 and 19. This single discontinuity in the Apollo 15 presunrise
temperature curves probably results from a spurious change in extraneous
EMF in the thermocouple circuitry. Otherwise, the data indicate that the
thermocouples are quite stable at night.

Factors Affecting Long-Term Temperature Variations of the Lunar Surface

1) The long-term variations in maximum surface temperature of a level surface element on the moon depend on the time variation of insolation and the lunar latitude of the element. The Appendix gives a derivation of solar flux at a fixed point on a smooth, spherical moon as a function of time. Figure 4B shows the lunation maxima of this function for the periods from July 1971 to October 1974 at Rima Hadley and from January 1973 to October 1974 at Taurus Littrow. The insolation at Taurus Littrow is more intense because that site is nearer the equator. The strong annual component results from the eccentricity of the earth's orbit. The amplitude modulation of this annual component results from the precession of the moon's spin axis with a period of 18. 6 years.

2) The small variation in presunrise temperature depends on the annual variation in total flux during the lunar day and the thermal inertia of the lunar regolith. There are two factors involved in determining total flux; The variation of insolation intensity and the variation of the length of the insolation period. In Figure 4A, the variation in the period from sunrise to sunset, based on Equation 11 of the Appendix, is shown and compared with the observed period determined from the thermocouples. The fractional variation in the length of the insolation period is much smaller than that of the insolation intensity, and, consequently, has a proportionately smaller

effect on the presunrise surface temperature variations. In Figure 5, the theoretical variation in presunrise surface temperature is shown based on the insolation function and a thermal model of the lunar surface (see References 1 and 2).

Notice that for presunrise temperatures the phase of the theoretical curve lags that of the annual insolation variation by about $\pi/4$ radians. This phase shift is expected because, for a semi-infinite solid, the variation of surface temperature lags a periodic variation in flux at the surface by exactly $\pi/4$ radians. See, for example, Reference 4, page 76.

Thermocouple Temperatures:

Thermocouples, buried inside a portion of cable exposed above the lunar surface, attain temperatures that provide radiative balance between impinging radiation from the sun and lunar surface and the cable's radiation to space and the lunar surface. This balance is expressed by:

$$T_c^4 = \frac{F_{cm}\,\epsilon_m\,a_{cir}\,T_m^4}{\epsilon_c} + \frac{a_{cs}\,s_n\,\sin\beta}{\pi\,\sigma\,\epsilon_c} + \frac{AF_{cm}\,a_{cs}\,s_n\,\cos\alpha}{\sigma\,\epsilon_c} \qquad (1)$$

The notation is the same as that used in Reference 2, except for s_n, the normally incident flux which is a function of time; α, the incident angle of solar radiation on the lunar surface; and β, the angle between the cable axis and impinging solar radiation. The absorptivities are denoted by small a's.

At lunar night $s_n = 0$ and the thermocouple temperature is

proportional to the lunar surface temperature.

During the lunar day $T_m^4 \cong s_n \cos \alpha (1-A)/\epsilon_m \sigma$. With

this assumption, the thermocouple temperature can be expressed solely as

a function of solar insolation and the angles α and β, i.e.,

$$T_c^4 = s_n \cos \alpha (K_1 \frac{\sin \beta}{\cos \alpha} + K_2) \qquad (2)$$

where all constants have been lumped into K_1 and K_2. This relation shows

that the variation of thermocouple temperature with variation of s_n is a

function of the angle of orientation of cable. For a vertically oriented

cable, for instance, $\alpha = \beta$ and

$$T_c^4 = s_n \cos \alpha (K_1 \tan \alpha + K_2) \qquad (3)$$

whereas for a horizontal, north-south oriented cable $\sin \beta = \cos \alpha$ at

lunar noon and

$$T_c^4 = s_n \cos \alpha (K_1 + K_2) \qquad (4)$$

Discussion of Measurements

Presunrise Temperatures

The amplitudes and phase lags of the presunrise temperatures

show no significant disagreement with those derived from the thermal model

of the lunar soil (see Figure 5B). The mean values of these temperatures,

for the exposed thermocouples at both sites, agree well with expected values

based on measurements of the thermal and radiative properties of the cables

and the lunar surface.

Lunar Daytime Temperatures

The long term modulations of the annual variation are due to the changes in the angles α and β as the moon precesses. Equations (2), (3) and (4) show how the cable orientation determines the shape of this modulating envelope for some special cases. Thermocouple 2, at Hadley Rille, which is approximately horizontal shows the same kind of modulation as the surface temperature (see Figure 5 and Equation 4). Thermocouple no. 4, at the same site, is in the projecting borestem and thus has an approximately vertical orientation. At lunar noon thermocouple no. 4 is in equilibrium with the borestem. Writing Equation (3) as

$$T_c^4 = K_1 s_n \sin \alpha + K_2 s_n \cos \alpha$$

shows that two modulations, 90° out of phase, are involved. The second term on the right defines the effect of heating by radiation from the lunar surface, which has an increasing envelope over the period of observation being discussed, while the direct solar heating of the cable element defined by the first term on the right, has a contracting envelope. The resulting envelope will be a sum of these terms, the exact shape depending on the mean value of α and the relative sizes of K_1 and K_2. Figure 3 B shows that there is only a very small modulation of thermocouple no. 4 temperatures, thus the two modulations appear to cancel.

A similar analysis, however, cannot explain the variation in the maximum temperatures of thermocouple no. 2 at Taurus Littrow. The lower temperatures of this sensor near perihelion 1974 (see Figure 3), compared with those near perihelion 1973, could possibly be accounted for by cable orientation. However, the same reasoning would require the temperatures near aphelion 1974 to be higher than those near aphelion 1973. The observed maximum temperatures, do not conform to this requirement. It is not certain that this anomalous behavior is significant, however, since the instrumental noise in this sensor near noon makes accurate temperature determinations difficult.

Besides the specific examples already discussed, there are some general patterns in the maximum temperature variations of the thermocouples which can be explained in terms of precession and cable orientations. It can be seen in Figure 5A that the phase of the maximum thermocouple temperatures lead maximum surface temperatures by various amounts up to 1 lunation. This is also true for all the thermocouples not shown in the figures. In fact, the maximum surface temperatures, which are in phase with the maximum insolation curve, maximize each year about a lunation after perihelion and minimize about a lunation after aphelion. This phase lag is caused by the northward advance of the sun near perihelion each year and the corresponding southward recession near aphelion due to the precessional motion, which, in addition to increasing the

amplitude of the annual variation, shifts the extrema of this variation to the right. Several years from now, when the amplitude of the annual wave is decreasing, the extrema will be shifted toward the left. The thermocouples are not as strongly affected by these precessional effects, because they are, in general, not north-south oriented so that the change in the angle β (in Equation 2) is not, in general, as large as the change in α. Thus, the direct heating of the thermocouples tends to maximize and minimize nearer to perihelion and aphelion respectively, causing the phase lead seen in the maximum thermocouple temperatures.

It has also been noted that there is a significant lack of symmetry in the modulating envelope of the average maximum temperatures of the Apollo 15 thermocouples, which implies a drift in the mean temperature of all these sensors. Precessional effects cannot account for a drift in mean temperature of the lunar surface, or a thermocouple junction; but, the observed drift can be removed by correcting for an apparent error, caused by the circuitry. The difference in temperature between junction 1 and the topmost platinum resistance thermometer in probe 1 near noon at both sites is shown in Figure 6B and D. The platinum sensor is assumed to be stable, while the relative temperature of junction 1 shows a steady upward drift through lunation 18, a sudden jump between lunations 18 and 19, and subsequently it is stable. The temperatures of thermocouples 2 and 4 at Hadley Rille, corrected for this drift are shown in Figure 5A. A similar correction for the temperatures of thermocouple 2 at Taurus Littrow has not

been made since it does not significantly change the anomalous behavior of this sensor.

Reference Thermometer Temperatures

In Figure 6A and C the maximum temperatures and the presunrise temperatures of the reference thermometer in the electronics box are shown for both experiments. Except for the anomalously high values in the second lunation at each experiment, caused by increased heating of the electronics box during conductivity experiments, the maximum temperatures show the annual variation superimposed on a gradual upward drift in mean temperature. At Apollo 15, this drift seems to be leveling after three years, whereas the period of observation at Apollo 17 is not sufficiently long to confirm a similar effect there. The similarity in the initial drift rates at the two sites suggests that this effect is characteristic rather than spurious.

The possibility that this drift in mean temperature is caused by a drift in calibration of the reference thermometers is considered unlikely for the following reasons. First, the reference thermometers are platinum resistance bridges similar in construction to those in the probe bodies which preflight tests showed to be extremely stable (Kleven et al., 1970). Next, thermocouple 1 has one junction thermally connected to the reference thermometer and the other inside the uppermost platinum resistance element in the probe. This provides direct comparison of the probe and reference bridge. The difference in temperature between thermocouple 1 and the uppermost platinum resistance thermometer at the Apollo 17 site (see Figure 6B) near noon shows

no long-term drift and indicates that the calibration of the reference thermo-meter in the Apollo 17 experiment is stable. Therefore, the upward drift shown in Figure 6A is a real change in mean temperature of the electronics box. At Hadley Rille (Apollo 15), the same stability is evident after lunation 19 (see Figure 6D), indicating that the slow increase in mean reference thermo-meter temperature is probably real. But, prior to lunation 19 at Hadley Rille there is a gradual upward drift of the temperature difference between thermo-couple 1 and the uppermost platinum resistance thermometer and an abrupt decrease occurs between lunation 18 and 19. It is impossible to tell whether these changes are due to changes in the reference thermometer calibration, or the changes in EMF of the thermocouple 1 circuit. If the reference thermo-meter readings are corrected assuming the thermocouple drift up to lunation 18 is entirely to reference thermometer calibration drift, then the resulting mean electronics box temperatures show a decrease with time and an abrupt change at lunation 19 which is unlikely. Consequently, we think that the reference thermometer temperatures are accurate as they are shown in Figure 6C, and that the characteristics of thermocouple 1 have changed.

The presunrise temperatures of the reference thermometers are thermostatically controlled, and thus, not determined by the radiative balance of the electronics box with its environment. The differences in presunrise temperature between thermocouple 1 and the uppermost platinum resistance thermometers are stable at both experiments, which lends more support to our assertion that the reference thermometers are stable to within a few tenths

of a degree over three years. Although the possibility of instrument instability cannot be ruled out entirely, for all of the reasons given above it appears that the upward drift of the reference thermometer temperature at noon is a real rise in electronics box temperature.

This slow increase in temperature with time has been observed by thermometers on other ALSEP experiments. However, the results from the heat flow experiment are probably the most accurate. The most obvious cause of this temperature rise is a gradual increase in the absorptivity-emissivity ratio of the surfaces of the electronics box with time. This could result either from a degradation of the painted surfaces of the electronics housing or from a slow accumulation of fine lunar dust on the outer surfaces of the housing. We certainly can exclude the possibility that it represents a general rise in lunar surface temperature.

Conclusions

Equation (1), used in conjunction with a finite difference model of the lunar regolith and the insolation function, can be used to explain the long term temperature variations of the exposed thermocouples at Apollo sites 15 and 17. These thermocouples experience strong annual variations in temperature with amplitude modulations due to the precession of the moon. The amplitude and phase of these modulations depend on cable orientation. The data presented here indicate no detectable secular drift in lunar surface temperature over the three year observation period.

In situ comparison of temperatures of three different types of thermometers indicates that the Heat Flow Experiment thermometers and detection circuits are stable to within a few tenths of a degree over the periods of observation, except for the drift in junction 1, probe 1, at Apollo 15. The gradual upward drift in the near-noon temperatures of the reference thermometers indicate a steady increase in electronics box temperature at the two sites. A likely explanation of this increase is an increase in the ratio of optical absorptivity to infrared emissivity of the surface of the electronics housing, due either to a slow accumulation of dust on the housing surfaces or a gradual degradation in the reflective properties of the paint on the housing.

References

Keihm, S. J., K. Peters and M. Langseth (1973) Apollo 15 measurement
of lunar surface brightness temperatures: Thermal conductivity
of the upper 1.5 meters of regolith; Earth Planet. Sci. Ltrs., v.
19, p. 337-351

Keihm, S. J. and M. Langseth (1973) Surface brightness temperatures
at the Apollo 17 heat flow site: Thermal conductivity of the upper
15 cm of regolith; Proc. Fourth Lunar Sci. Conf., in, Geochim.
et Cosmochim. Acta Suppl. 4, p. 2503-2513

Langseth, M. G., S. J. Keihm and J. L. Chute (1973) Heat flow experiment,
Section 9 of Apollo 17 Preliminary Science Report NASA SP-330

Carslaw, H. S. and J. C. Jaeger (1959) Conduction of Heat in Solids,
Second Edition, Oxford, Clarendon Press, 510 pgs.

Kleven, Lowell, L. Lofgren and P. Felsenthal (1970) A rugged, stable
platinum resistance thermometer; The Review of Scientific
Instruments, v. 41, n. 4, p. 541-544

*

TABLE 1

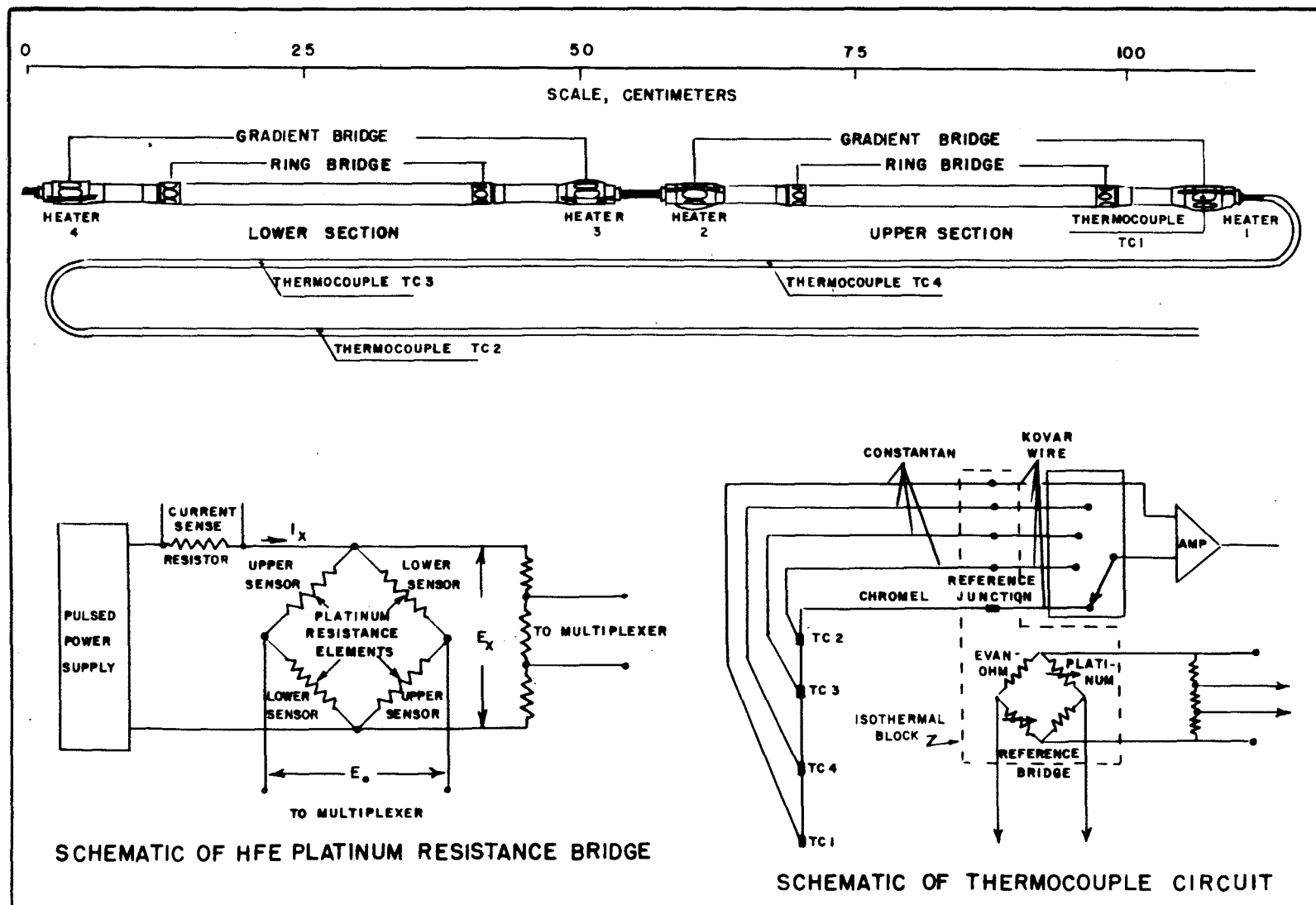| Thermometer	Absolute Temperature	
	Range, °K	Accuracy °K
Platinum Thermometers	190 to 270	±0.05
Thermocouples	70 to 400	±0.70
Thermocouple Reference Thermometer	253 to 363	+0.01

Figure 1 - Lunar heat flow experiment temperature probe and temperature measuring circuits.
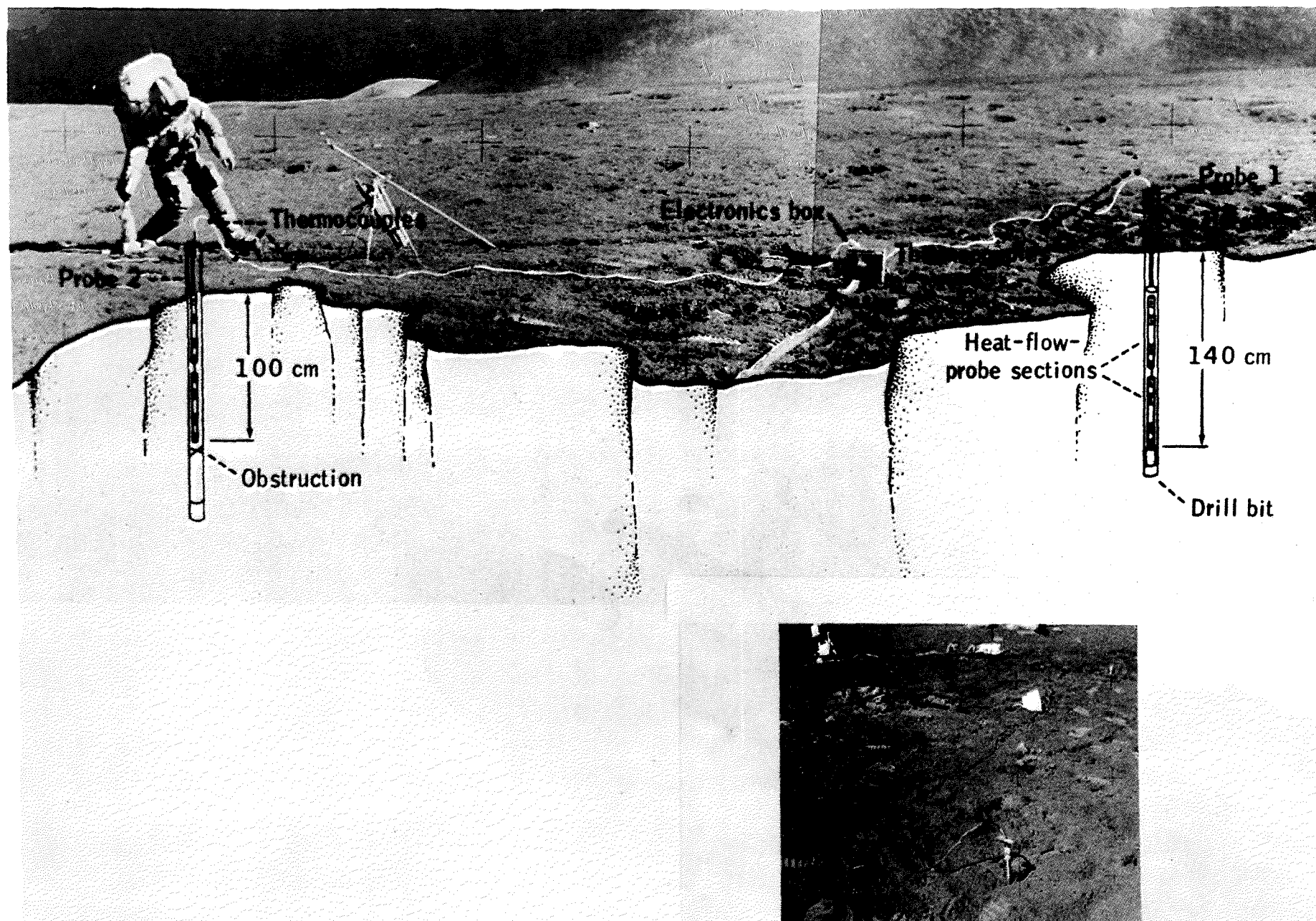
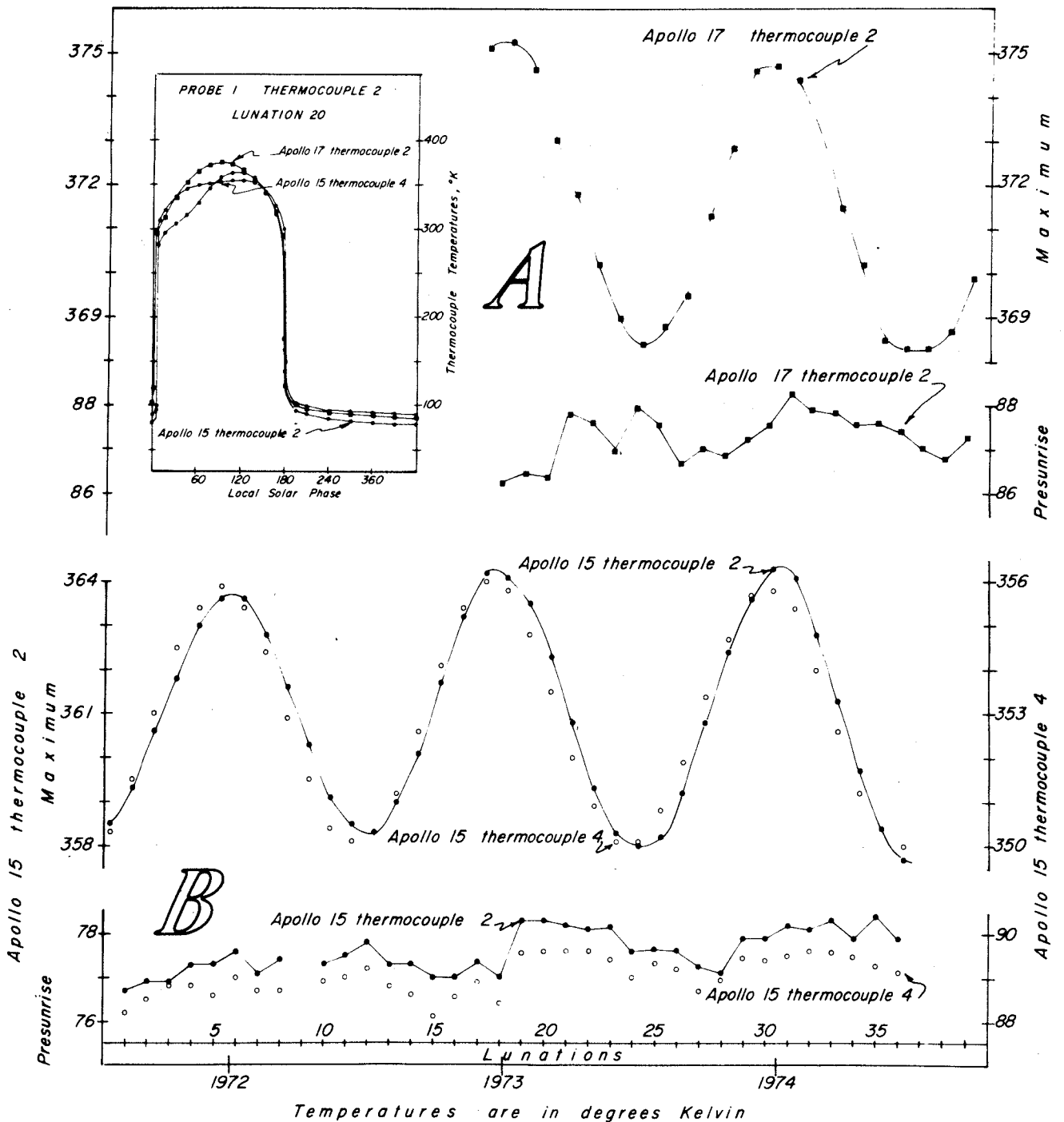Figure 2 - Probe emplacement at Apollo sites 15 and 17.

Figure 3 - Inset; three thermocouple temperature variations for a typical lunation; A-maximum and presunrise temperatures for a thermocouple above the surface at Taurus Littrow; B-similar data for two thermocouples at Hadley Rille; thermocouple 4 is located inside the borestem projecting above the surface.
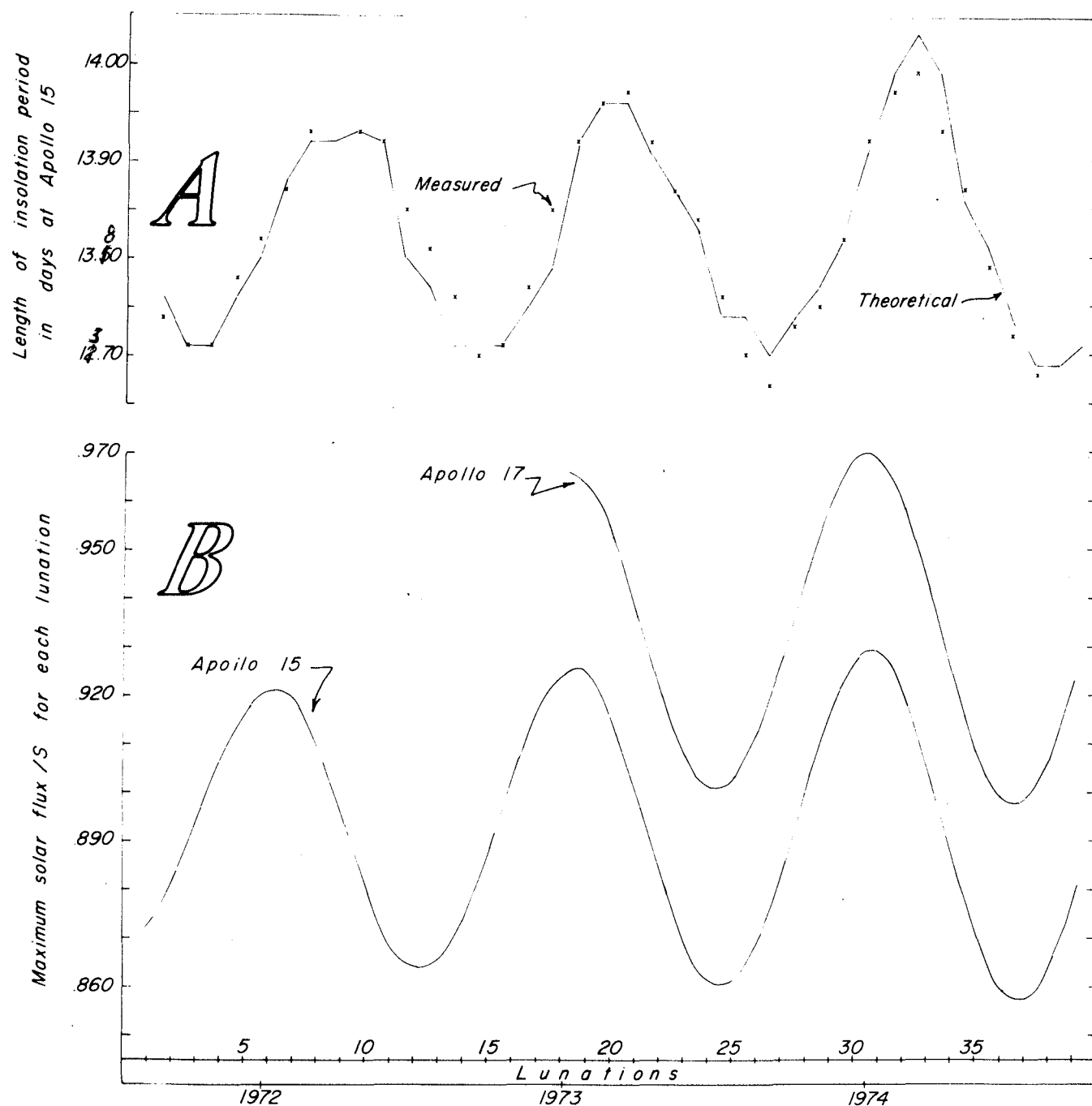
Figure 4 - A; the variation in insolation period length at Hadley Rille as predicted by the insolation function derived in the Appendix (Eq. 11) and compared to the observed length based on abrupt changes in thermocouple temperatures - B;theoretical variation in insolation intensity maxima at Apollo 15 and 17 sites.
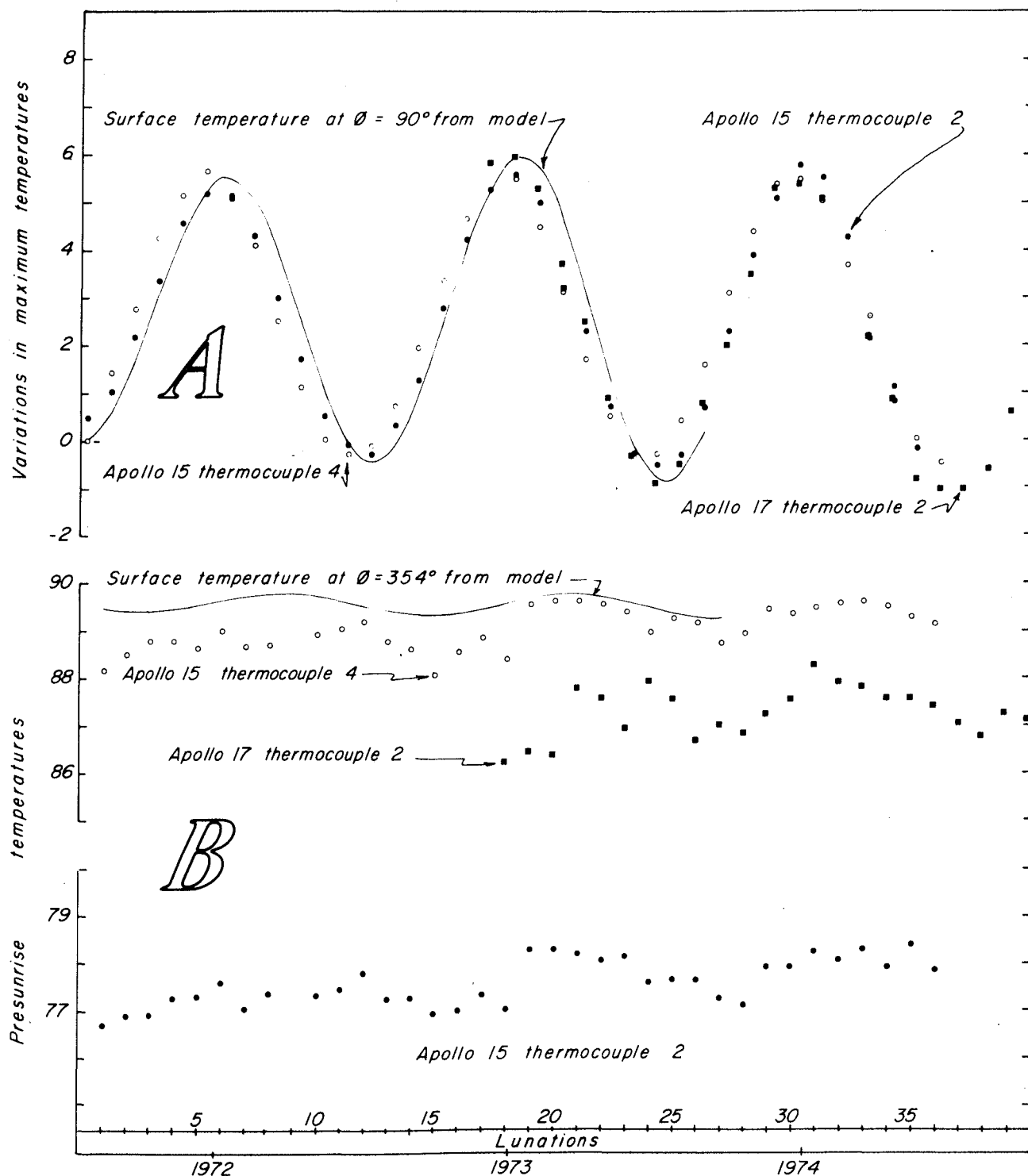
Figure 5 - A; maximum thermocouple temperatures compared with lunar surface temperatures predicted by the insulation function and a thermal model of the lunar regolith - B; theoretical and observed presunrise temperatures.
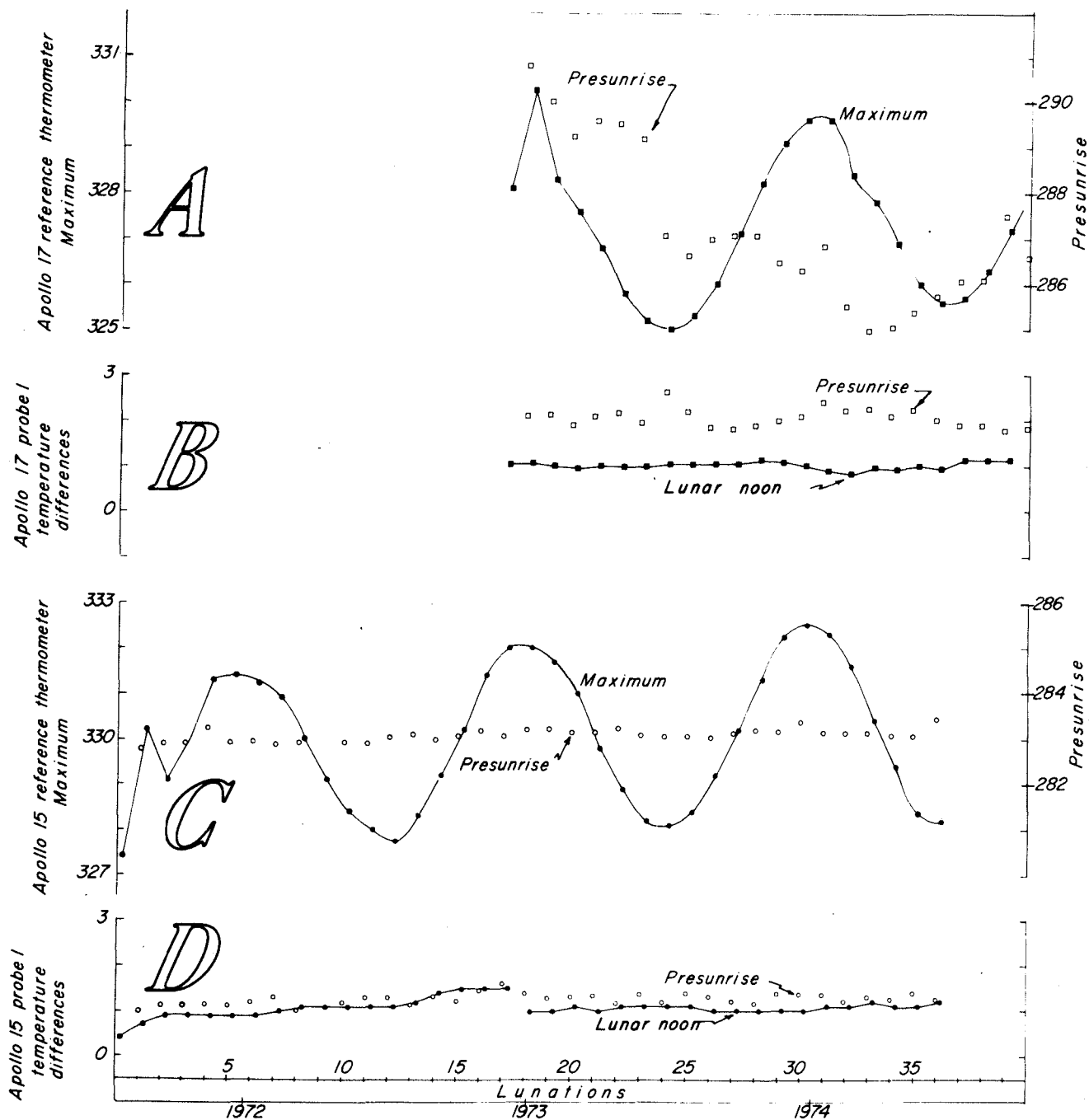
Figure 6 - A; maximum and presunrise reference thermometer temperatures at Taurus Littrow - B; temperature difference between thermocouple 1 and the uppermost platinum resistance thermometer in probe 1 at Apollo 17 near noon (maximum) and just before sunrise - C and D; similar observations at Hadley Rille.

APPENDIX

LUNAR INSOLATION FUNCTION

I.   Motions Considered

A simple expression for the solar flux at any point on the surface of a smooth, spherical moon has been derived, based on four idealized motions:

1) Annual revolution of the earth around the sun, assumed to be Keplerian and counterclockwise;

2) Synodic revolution of the moon around the earth, assumed to be uniform circular and counterclockwise in the ecliptic plane;

3) Uniform rotation of the moon upon its spin axis, counterclockwise with a Draconitic period (the interval between two successive transitions of the moon at its ascending node); and,

4) Uniform precession of the spin axis about a normal to the ecliptic plane at a constant angle of 1.5°, clockwise with a period of 18. 6 years.

II.   Derivation

The flux s on a unit surface area perpendicular to $\vec{u}_A''$ at A" (see Figure A1)   is equal to the flux on a unit area normal to the sun line

$\vec{u}''_s$ which is considered to be parallel to $\vec{u}_s$, times the cosine of the angle $\propto$ between $\vec{u}''_s$ and $\vec{u}''_A$:

$$s = s_n \cos \propto .$$

s_n depends only on the distance of the moon from the sun. Cos $\propto$ is equal to the projection of $\vec{u}''_A$ into $\vec{u}_s$.

A. Determination of s_n.

$$s_n = Q/R_M^2 \qquad (1)$$

where Q is the source strength of the sun and R_M is the sun-moon distance (see Figure A2). By the law of cosines

$$R_M^2 = R_E^2 + r^2 - 2R_E r \cos \psi$$

$$= R_E^2 \left(1 + \left(\frac{r}{R_E}\right)^2 - 2\left(\frac{r}{R_E}\right) \cos \psi \right)$$

Since $\frac{r}{R_E} \approx \frac{.25}{93} \approx .0027$, the square of this ratio will be ignored, and

$$R_M^2 \cong R_E^2 (1 - .0054 \cos \psi) \qquad (2)$$

R_E can be written as

$$R_E = a(1 - e \cos \xi)^* \text{ where} \qquad (3)$$

*see for example, W. M. Smarts Textbook on Spherical Astronomy

a is the length of the semi-major axis of the earth's orbit, e is the eccentricity of the earth's orbit, and ξ is the earth's eccentric anomaly, which can be expanded in terms of the eccentricity and the mean anomaly $\mathcal{M}$ as

$$\xi = \mathcal{M} + (e - e^3/8)\sin\mathcal{M} + 1/2\ e^2 \sin 2\mathcal{M} + \dots\dots$$

(for t, in mean solar days, $\mathcal{M} = 2\ (t - t_p)/T$, and $T \cong 365.25$ days. The subscript p refers to perihelion). Since e is about .017, terms involving higher powers of e than the first will be ignored. So

$$\xi \cong \mathcal{M} + e \sin \mathcal{M} \tag{4}$$

combining (3) and (4) gives

$$R_E \cong a(1 - e\cos(\mathcal{M} + e\sin\mathcal{M}))$$
$$= a(1 - e(\cos\mathcal{M}\cos(e\sin\mathcal{M}) - \sin\mathcal{M}\sin(e\sin\mathcal{M})).$$

Squaring both sides, noting that $\cos(e\sin\mathcal{M}) \cong \cos e = 0.99986$ and $\sin(e\sin\mathcal{M}) \cong e\sin\mathcal{M}$, and dropping the term in e^2 leaves

$$R_E^2 \cong a^2(1 - 2e\cos\mathcal{M}). \tag{5}$$

Combining (2) and (5) gives

$$R_M^2 \cong a^2(1 - 0.034\cos\mathcal{M})(1 - 0.0054\cos\psi)$$

and from (1)

$$s_n \cong \left(\frac{Q}{a^2}\right)\ \frac{1}{(1 - 0.034\cos\mathcal{M})(1 - 0.0054\cos\psi)}$$

Since 0.034 and 0.054 are both small compared to 1, and the product is less than e^2, s_n can be sufficiently approximated as

$$s_n \stackrel{\sim}{=} \left(\frac{Q}{a^2}\right)(1 + 0.034 \cos \mathcal{M} + 0.054 \cos \psi)$$

using the expansion $1/1 - x = 1 + x - x^2/2 + \ldots\ldots\ldots$.

If we define S as Q/a^2, which is approximately the mean flux over a year (the solar constant), then

$$s_n \stackrel{\sim}{=} S(1 + 0.034 \cos \mathcal{M} + 0.0054 \cos \psi) \tag{6}$$

B. Determination of Cos α

As the moon rotates on its spin axis, the point A'' describes the circle shown in Figure 1. Figure A3 shows this circle projected onto the ecliptic plane along O'O''Z'. The semi-minor axis of the ellipse lies along O O', and the semi-major axis along O'X'. The length of the semi-major axis is $\sin \lambda$ which is the length of the vector $\vec{\rho}$ ''. The length of the semi-minor axis is $\sin \lambda \cos \theta$. Considering the sun to be infinitely distant,

$$\cos \alpha = \rho \cos (\phi + \beta) \tag{7}$$

where ρ denotes the length of $\vec{\rho}$ and ϕ and β are as shown.

Expanding (7) yields

$$\cos \alpha = \rho(\cos \phi \cos \beta - \sin \phi \sin \beta) \tag{8}$$

From Figure A3, $\cos \beta = x/\rho = \rho''\cos \omega / \rho = \sin \lambda \cos \omega/\rho \tag{9}$

and $\sin \beta = y/\rho = (\Delta y + y')/\rho = (\cos \lambda \sin \theta + \sin \lambda \cos \theta \sin \omega)/\rho \tag{10}$

By (8), (9), and (10)

$$\cos \propto = \cos \phi \sin \lambda \cos \omega - \sin\phi\cos\lambda \sin\theta - \sin\phi\sin\lambda \cos \theta \sin \omega$$

$$\cong \sin \lambda (\cos\phi\cos \omega - \cos\theta\sin\phi\sin \omega - \cot \lambda \sin\theta\sin\phi)$$

$$\cong \sin\lambda (\cos(\phi + \omega) - \cot\lambda \sin\theta \sin\phi) , \tag{11}$$

since $\cos \theta (\cong 0.99966)$ is nearly 1.

C. The Angle ϕ

ϕ depends on the earth's true anomaly, v, the correction to this anomaly for the moon's revolution about the earth, Δv (see Figure A2), and the precession γ . v can be expanded in terms of $\mathcal{M}$ and e as

$$v = \mathcal{M} + (2e - \frac{1}{4} e^3) \sin\mathcal{M} + \frac{5}{4} e^2 \sin 2\mathcal{M} + \ldots$$

$$\cong \mathcal{M} + 2e \sin \mathcal{M} \tag{12}$$

to the same approximation used for E in equation (4).

By the law of sines (in Figure 2)

$$\frac{r}{- \sin \Delta v} = \frac{R_M}{\sin \psi} \qquad \text{or } \sin\Delta v = - r \sin \psi / R_M$$

Substituting for R_M from (2) and using $\sin \Delta v \cong \Delta v$,

$$\Delta v \cong - 0.0027 \sin \psi \tag{13}$$

to the level of approximation being used.

Letting the subscript 0 denote initial values

$$\phi = \phi_0 - (v - v_0) + 0.0027 \sin(\psi - \psi_0) - (\gamma - \gamma_0) \tag{14}$$

using (13), with v given by (12) and where ψ and γ are as described in I.

III.   Time Origin and Initial Conditions

Since the eccentric anomaly ξ and the true anomaly v are computed from perihelion, it is convenient to use the occurrence of perihelion on January 2.50, 1973 as a time origin. Thus, $v_0 = 0$. The value of ϕ_0 can then be calculated by noting that $\phi = 0$ when the sub-solar point crosses the moon's equator going north, which occurred in 1973 on January 8.65, and that $\psi = 0$ at new moon which occurred on January 4.67. γ can be arbitrarily set to $\gamma_0 = 0$ at perihelion 1973. Using values from the American Ephemeris and Nautical Almanac (14) becomes

$$\phi = 0.112 - v(t - t_0) + 0.0027 \sin(\psi(t - t_0) - 0.46) - \gamma(t - t_0)$$

measured in radians with t in mean solar days.

The initial value for ω is the difference in selenographic longitude between the point A and the sun at $t = t_0$. From the Almanac

$$\omega_0 = 4.20 - \text{col}_A$$

where col_A denotes the selenographic colongitude of A.

IV. Comparison with Apollo Data

The roots of the expression inside the parentheses of equation (11) correspond to sunrise and sunset times on a smooth, spherical moon. These times can be compared with sunrise and sunset times determined from the exposed thermocouples at the Apollo 15 and 17 sites. They agree within the limits of accuracy of the topographic corrections. The intervals between consecutive sunrises as predicted by equation (11) differ in a random way (no systematic error) from the intervals determined from the thermocouple data over the times the experiments have been in operation with a standard deviation of 0.028 days or about 40 minutes. The thermocouple data are sampled about every hour, which would give a standard deviation of about 0.017 days, or about 24 minutes, assuming that the errors in estimation of these sunrise times are uniformly distributed over an hour interval. The other 16 minutes are assumed to be due to the effects of topography and possibly to inaccuracies in the determination of the initial angles.
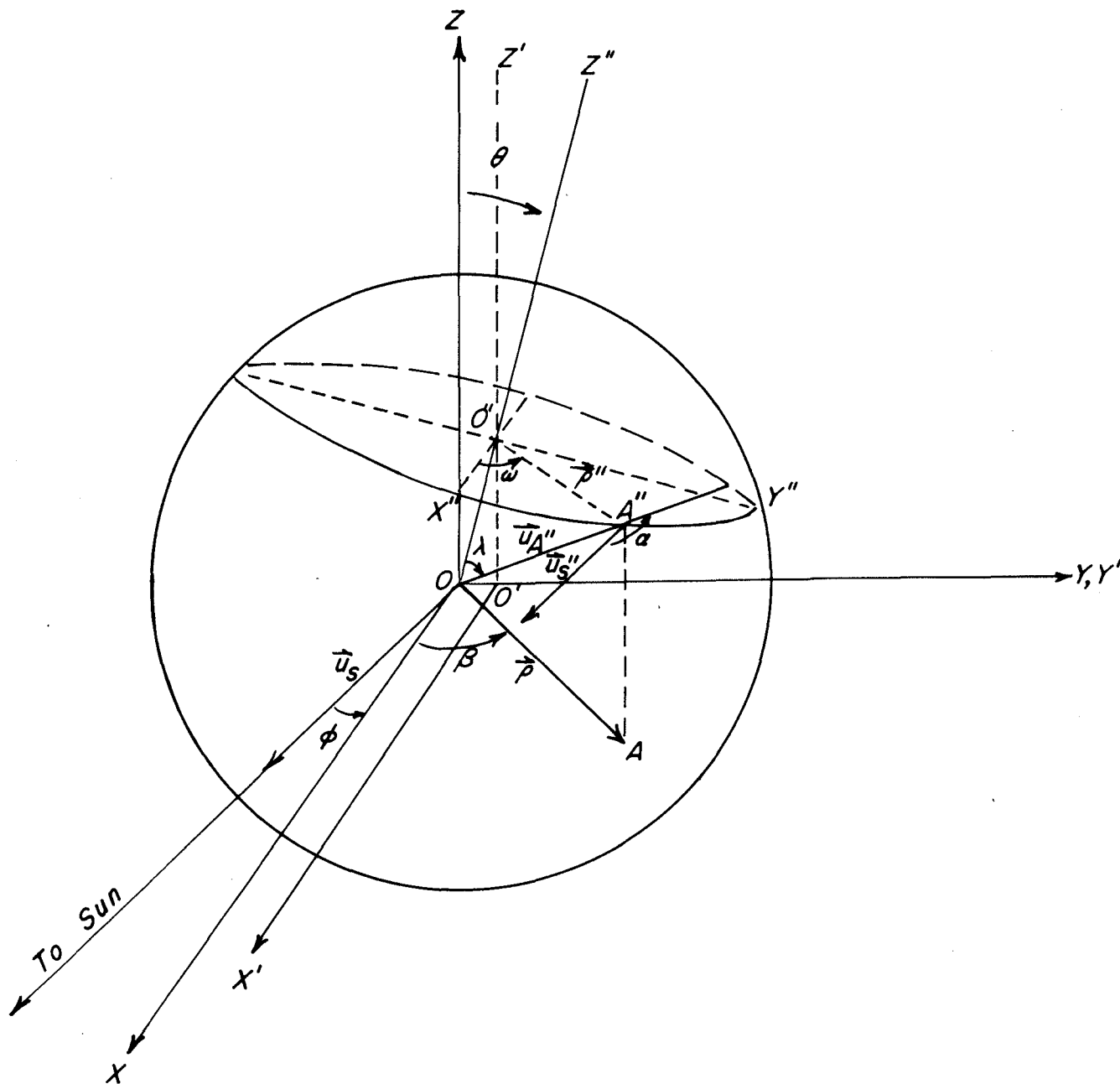
Figure A I

The moon's spin axis (OO''Z'') is inclined at a constant angle θ with respect to OZ which is normal to the ecliptic plane. O'O''Z' is parallel to OZ. OS ($\vec{u_s}$), OX, O'X', OO'Y(Y'), and OA ($\vec{P}$) all lie in the ecliptic plane. The angles φ and β are measured in this plane. The lines OX, O'X' and O''X'' are considered to be mutually parallel; $\vec{u_s}$ and $\vec{u_s}''$ are considered coplanar and parallel; therefore, ∝ is the angle measured from $\vec{u_s}$ to $\vec{u_A}''$ also. (The sun is assumed to be infinitely distant for these approximations.) λ is the colatitude of the point at A'' measured from the North Pole. The $\vec{u}$'s are unit vectors.
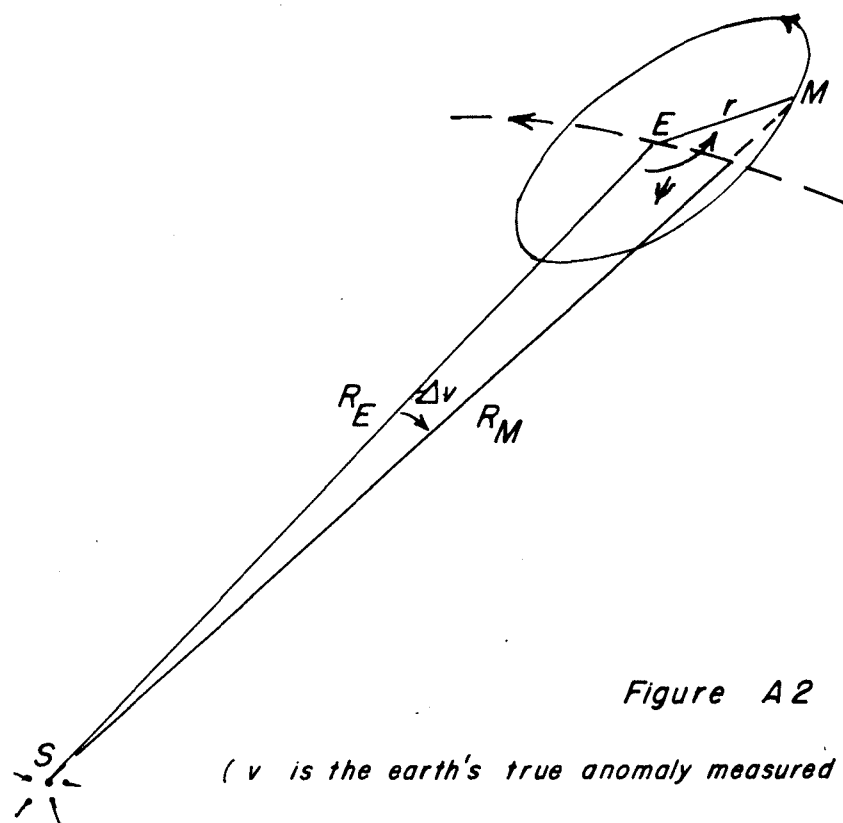
Figure A2

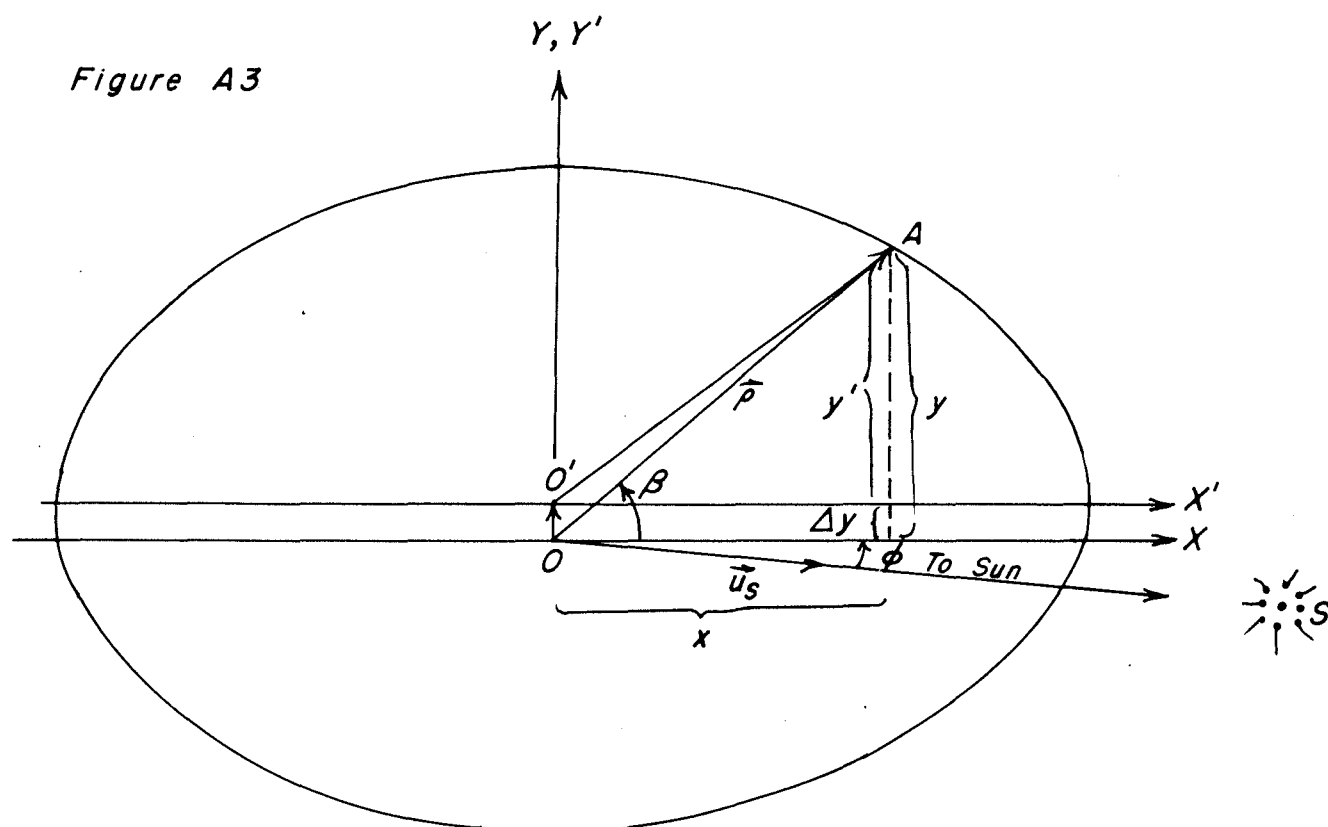(v is the earth's true anomaly measured from perihelion)

Figure A3